

Louis J. Wicker² and David C. Dowell^{1,3}¹ Cooperative Institute for Mesoscale Meteorological Studies, Univ. of Oklahoma, Norman, OK²NOAA/ NSSL, Norman, OK

1. INTRODUCTION

Part III in this series of papers discussing the F4 tornadic supercell of 8 May 2003 uses Doppler radar observations of reflectivity and radial velocity to initialize a high-resolution numerical cloud simulation of the storm. The unique aspect of this work is that for the first time a large-eddy-type simulation of a severe storm will be initialized from an analysis generated by the convective-scale ensemble Kalman filter data assimilation analysis presented in Part II by Dowell et al. (2004, SLS preprint paper **12.5**, hereafter known as DWS04). The grid mesh parameters are somewhat coarser than those used in Wicker et al. (2002), i.e., these simulations use grid resolutions on the order of 100-200 m, which still should resolve a large portion of the turbulent eddy structures within the storm. By employing such a fine grid mesh it is hoped that the error associated with parameterization of turbulent eddies is minimized. High resolution is also required to capture the gross features of any tornado-like vortex that might form in the simulation.

By employing high-resolution horizontal and vertical meshes within the three-dimensional EnKF storm-scale analysis, we will generate a storm-scale simulation that at least initially, represents a "best estimate" of the observed storm. This methodology is being proposed as a possible analysis technique for convective scale observations from several field programs (e.g., BAMEX and VORTEX-II). The simulated storm will be closely compared to the available observations from nearby radars (not used in the data assimilation) as well as other available in situ measurements in order to evaluate the forecast accuracy of the experiment.

Single Doppler observations of the supercell are presented in Part I by Burgess (2004, SLS preprint paper **12.4**, hereafter known as B04). DWS04 presents the analysis and forecast storm simulation and compares these with the observational data. DWS04 employed a coarser analysis and forecast grid having 1 km horizontal resolution. Here our high-resolution simulation is examined again relative to the observations shown in B04 to determine if there is added value with a higher resolution forecast. These comparisons include a comparison of time-height diagrams, timing and vertical structure of low-level vortex in the simulation etc. While it is unlikely that the simulated storm will closely match the observations for a long period of time or in such fine detail, the success of EnKF assimilation scheme for convective storm analysis

has encouraged us to attempt a more detailed forecast so that we can evaluate the potential usefulness of this approach.

2. EXPERIMENTAL DESIGN

DWS04 describes in detail the approach and methodology used to create the analysis and forecast of the 8 May 2003 Oklahoma City tornadic supercell. The reader can also refer to recent research in EnKF data assimilation for radar data (Snyder and Zhang 2003; Zhang et al. 2004; Dowell et al. 2004; Tong and Xue 2004) for a more detailed discussion of the convective scale ensemble Kalman filtering methodology. Here we highlight the procedure used to initialize and run the high-resolution simulation beginning from the lower-resolution analysis:

- As in DWS04, the mean analysis fields at 2126 UTC are created from a 50-member ensemble at a horizontal resolution of 1 km over the 150x150 km domain.
- The analysis fields (e.g., the full model fields, u , v , w , pressure, etc.) are then horizontally interpolated to a 75x75 km domain having a horizontal grid spacing of 250 m.
- The vertical resolution remains unchanged: 60 vertical levels with a low-level grid spacing of 100 m through a depth of 1 km, stretching to 700 m near the top of the domain.
- Unlike the original forecast, the high-resolution domain grid is translated at $u=14$, $v=8$ m s^{-1} to keep the storm near the center of the smaller domain.
- The lower boundary remains the same (free slip) as do all other model parameters except for the time step, which is set to 3 seconds.
- The simulation is integrated forward in time for 40 minutes to 2206 UTC, which is when the tornado was observed to touchdown in the southwestern portions of Oklahoma City.

The simulations shown here use a horizontal grid spacing of 250 m. Based on the results (see below), it is not clear whether higher grid resolutions (~100 m) will be useful. Additional work addressing this issue will be shown during the presentation at the conference.

3. RESULTS

3a. Lifecycle

Figure 1 shows the observed reflectivity, the reflectivity from the 1 km resolution forecast (from DWS04) and the high-resolution reflectivity forecast after 38 minutes (2204 UTC). The three images are created from interpolating the data (from KOUN, the 1 km grid, or the 250 m grid) to a 1 km horizontal mesh. Both forecasts show similar features to the observed reflectivity (Fig. 1a). Both forecasts show the splitting on the left flank of the main storm that was observed in the real storm.

minute forecast period, and therefore the echo morphology is more complicated than in the 1 km forecast and (apparently) in the observed storm.

During the forty minute forecast period, the supercell in the high-resolution simulation generates two distinct circulations. By 2204 UTC, the original circulation has occluded and is now located near the southwest end of the echo (e.g., “C1” in Figure 1c). The second circulation is associated with the hook echo farther northeast along the edge of the storm (e.g., “C2” in Figure 1c). The low-level vorticity fields (not shown) support this hypothesis. Early on in the forecast the horizontal fields readjust to the new grid resolution,

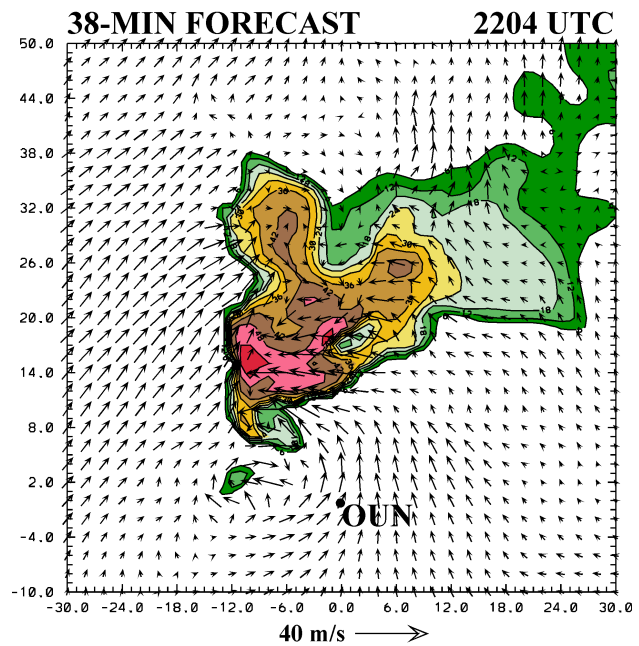
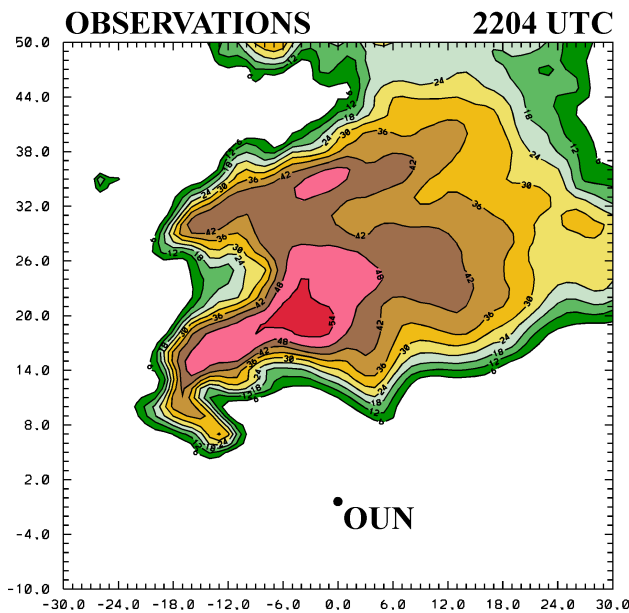
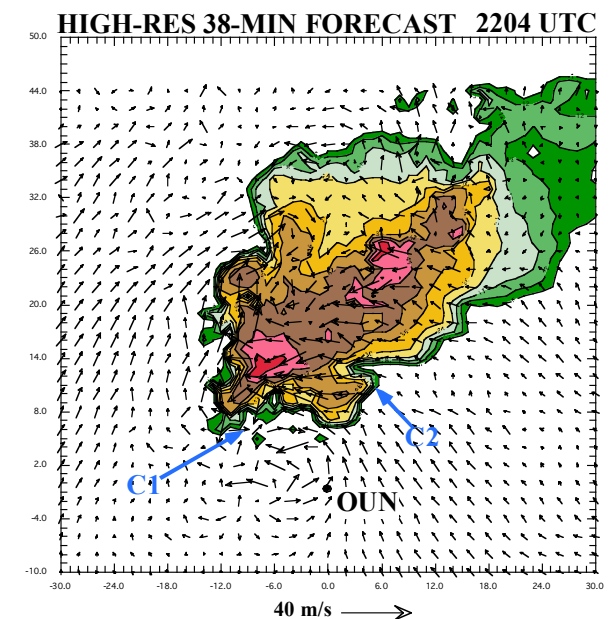


Figure 1. (a) Observed (above), (b) 1 km model-forecast (top-right), and (c) 250 m model-forecast (bottom-right) reflectivity (contours and shading at intervals of 6 dBZ₀) at 2204 UTC at 2.0 km AGL in a 60 km × 60 km sub-domain. Horizontal storm-relative winds in the model are also shown. C1 and C2 refer to the two circulations described in the text.

Neither storm shows the northeast-southwest band of very high reflectivity evident in the observed storm and the areal extent of the observed reflectivity is somewhat larger than both forecast storms.

The structure of the high-resolution simulation differs more from the observed reflectivity than does the 1 km forecast. There are several reasons for this. First, the high-resolution forecast grid has 16x more information than the 1 km grid. Even with the smoothing associated with the interpolation, the high resolution has more detail. A better comparison for model output having these resolutions may be to interpolate the model data to the radar grid directly and compare the fields (we plan to do this). Another factor is that the high-resolution simulation is more complicated in its evolution than its lower resolution counterpart. The high-resolution simulation spins up several circulations during the forty-



and this process takes several minutes. As this readjustment is happening (~2234 UTC) a mesocyclone begins to form near cloud base and intensifies. This is associated with only a moderately strong surface circulation. By 2250 UTC this circulation has occluded and a new center of circulation has developed further east. Beneath cloud base this circulation eventually becomes stronger than the first, and peak vorticity values ($\zeta > 0.1 \text{ s}^{-1}$) are seen for several minutes in the surface fields. However, the “cycling” of the second circulation occurs prior to the observed tornadogenesis, and by 2204 UTC the second spinup is decreasing in intensity. Also, the size of the overall modeled circulation is smaller in scale than the observed circulation from the KTLX radar.

The evolution of the high-resolution forecast, at least at low-levels, appears to be strongly controlled by the development of a strong cold pool beneath the storm's precipitation region (not shown). Despite the presence of strong vertical shear present in the background environment, a significant cold pool develops and pushes southward relative to the mid-level updraft motion. Our hypothesis is that the simulation cold pool is too strong relative to the observed storm's cold pool. This has two effects: the outflow initially spins up the low-level mesocyclone too quickly through baroclinic processes (Wicker and Wilhelmson 1995; Alderman et al. 1999) and then soon after “undercuts” the low-level circulation, causing its demise. This cycle repeats itself again in circulation “C2”. At the end of the forty-minute integration almost two full mesocyclone lifecycles have been completed. Therefore an entire circulation lifecycle is ~20 minutes or less in the simulated storm. The observed storm appeared to have a single long-lived mesocyclone that persists for nearly an hour aloft and with strong rotation near the surface for over the last 40 minutes (coincident with the tornado, B04).

3b. Time height plots

Figure 2 shows the time-height vorticity diagrams for the observed storm, the 1 km and high-resolution vertical vorticity fields. In a 50 km region centered on the storm, each model level is searched for the maximum ζ and a column of maximum vertical vorticity values is created for each time. Model output is generated at one-minute intervals.

As discussed in B04, the intensification of rotation in the OKC supercell first occurred aloft after 2130 UTC and then appeared near the surface around 2200 UTC. Figure 1b, from the 1 km run, shows a somewhat surprising similar evolution, with the development of a mesocyclone aloft after 2130 and the appearance of strong low-level rotation at the surface at 2202 UTC. In contrast, the 250 m simulation appears to have a very different evolution, with the development of a deep mesocyclone from the surface to 8 km aloft around 2135 UTC, and then a shallower circulation developing around 2159 UTC. These correspond to the two mesocyclone circulations discussed in the previous

section that develop and occlude rather quickly, relative to the observations and the 1 km simulation.

4. CONCLUDING REMARKS

The apparent differences shown between the two forecasts (and the observations) highlight many of the important and unresolved issues associated with convective storm-scale forecasts:

- The apparently more accurate forecast by the 1 km simulation indicates that high-resolution forecasts may not be able to be derived using a lower resolution analysis as the initial data. Adlerman and Droegemeier (2002) have also documented significant sensitivity in modeled mesocyclone behavior relative to changes in simulation parameters such as grid resolution. It is also equally possible that at higher grid resolutions, model error may grow more rapidly and contaminate the forecast more quickly than at lower grid resolutions.
- Due to a lack of radar observations near the surface, the storm's cold pool characteristics are almost completely determined by the model's microphysics parameterization. We believe that the microphysics parameterization is the major, if not dominant source, of model error. Dowell et al. (2004) discusses the importance of this issue more completely. This is a critical issue, since the characteristics of the cold pool control much of the storm's low-level and rotational evolution and the skill any model forecast can have in predicting low-level evolution is therefore directly related to the most significant source of model error. In this case, the microphysics scheme generates a cold pool that becomes quite strong and eventually undercuts the storm's updraft soon after 2204 UTC. This occurs in both low- and high-resolution simulations.
- Additional experiments were conducted that attempt to moderate the development of a strong cold pool by altering the hail density and intercept parameters in the microphysics scheme. These analysis and forecast experiments showed a strong sensitivity to even moderate changes in the parameters (Gilmore et al. 2004). For example, changing the hail intercept from 4×10^4 to 4×10^6 and reducing the hail density from 900 to 400 kg m^{-3} resulted in an analysis and forecast storm having a very weak cold pool. Subsequently, low-level mesocyclone formation did not occur.

While we believe that the experiments shown here are encouraging, the results clearly show several significant problems we believe to be associated with model error and/or the limits of the microphysical parameterization scheme. These will be investigated more thoroughly in the near future and hopefully some additional insights into these issues can be discussed at the conference.

Acknowledgements: We wish to thank discussions with Chris Snyder and Bill Skamarock of NCAR for helping us develop and use the EnKF methodology. Thanks to Kim Elmore for a review of this paper. Support for Dr. Dowell and this work was partially supported by NSF ATM-0333872 and NSF grant EEC-0313747 to the Engineering Research Center for Collaborative Adaptive Sensing of the Atmosphere. We also thank the NOAA-OU Cooperative Agreement #NA17RJ1227.

REFERENCES

Adlerman, Edwin J., Droegemeier, Kelvin K., Davies-Jones, Robert. 1999: A Numerical Simulation of Cyclic Mesocyclogenesis. *J. Atmos. Sci.* **56**, 2045–2069.

Adlerman, Edwin J., Droegemeier, Kelvin K. 2002: The Sensitivity of Numerically Simulated Cyclic Mesocyclogenesis to Variations in Model Physical and Computational Parameters. *Mon. Wea. Rev.* **130**, 2671–2691.

Dowell, D. C., F. Zhang, L. J. Wicker, C. Snyder, and N. A. Crook, 2004: Wind and temperature retrievals in the 17 May 1981 Arcadia, Oklahoma, supercell: Ensemble Kalman filter experiments. *Mon. Wea. Rev.*, **132**, 1982-2005.

Gilmore, M. S., J. M. Straka, and E. N. Rasmussen, 2004: Precipitation and evolution sensitivity in simulated deep convective storms: Comparisons between liquid-only and simple ice and liquid phase microphysics. *Mon. Wea. Rev.*, **132**, 1897-1916.

Snyder, C., and F. Zhang, 2003: Assimilation of simulated Doppler radar observations with an ensemble Kalman filter. *Mon. Wea. Rev.*, **131**, 1663-1677.

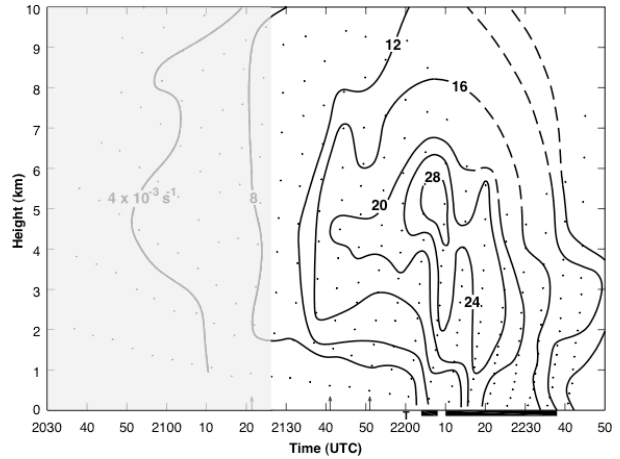
Tong, M., and M. Xue, 2004: Ensemble Kalman filter assimilation of Doppler radar data with a compressible nonhydrostatic model: OSS Experiments. *Mon. Wea. Rev.*, in review.

Wicker, L. J., and R. B. Wilhelmson, 1995: Simulation and analysis of tornado development and decay within a three-dimensional supercell thunderstorm. *J. Atmos. Sci.*, **52**, 2675-2703.

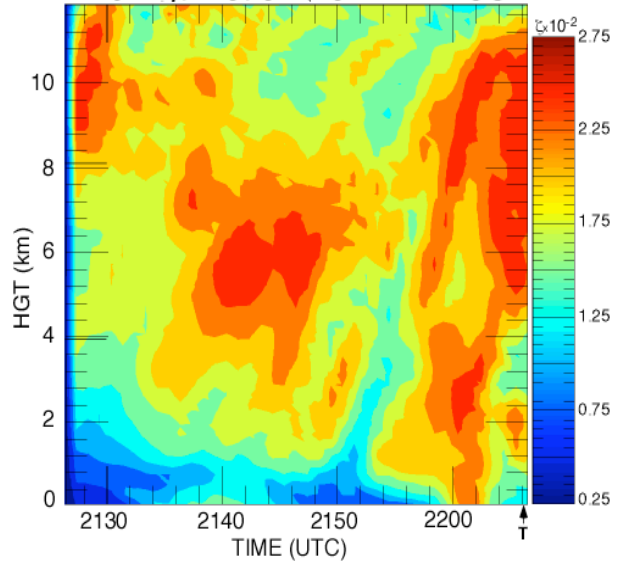
Wicker, L. J., R. B. Wilhelmson, D. Dowell, Y. Richardson, 2002: A large eddy simulation of a tornadic supercell: Comparison with observations. *Preprints, 21st Conf. on Severe Local Storms*, San Antonio, TX, Amer. Meteor. Soc., 262-263.

Zhang, F., C. Snyder, and J. Sun, 2004: Impacts of initial estimate and observation availability on convective-scale data assimilation with an ensemble Kalman filter. *Mon. Wea. Rev.*, **132**, 1238-1253.

Figure 2. (a) Observed time-height diagram of azimuthal vorticity (top-right). T and dark bars indicate tornado times while arrows indicate cell changes. Beginning of non-shaded region corresponds to the beginning of the model forecasts. From B04. (b) 1 km simulation forecast time-height diagram of vertical vorticity (middle-right), and (c) 250 m model simulation forecast time-height diagram of vertical vorticity (lower-right). Note the vorticity scale changes between (b) and (c) due to resolution differences.



Time-Hgt Plot of ζ for 1 km FCST



Time-Hgt Plt of ζ for 250 m FCST

